Available online at www.sciencedirect.com
ScienceDirect
Thin Solid Films 516 (2008) 6808–6812
www.elsevier.com/locate/tsf

Simulating performance of solar cells with spectral downshifting layers

W.G.J.H.M. van Sark

Department of Science, Technology and Society, Copernicus Institute for Sustainable Development and Innovation, Utrecht University, Heidelberglaan 2, 3584 CS Utrecht, the Netherlands

Available online 15 December 2007

Abstract

In order to estimate the performance of solar cells with downshifters under realistic irradiation conditions we used spectral distributions as they may be found outdoors. The spectral distributions were generated on a minutely basis by means of the spectrum simulation model SEDES2, using minutely measured data for global, direct, and diffuse irradiation from a Dutch meteorological station. Hourly aggregated spectra for a number of typical days (clear summer day, cloudy summer day, clear winter day, cloudy winter day) were used in modelling the output of the solar cell with and without downshifter. It was found that the simulated short current enhancement, which varies between about 7 and 23%, is linearly related with the average photon energy of the spectra.

Keywords: Spectrum conversion; Solar cells; Modelling

1. Introduction

Performance of solar cells can be enhanced by improved matching of the solar spectrum with the spectral response of the solar cells. Stacking multiple solar cells on top of each other, each sensitive to a different part of the solar spectrum, has proven to be a feasible solution. Conversion efficiencies of over 32% have been reached for a GaInP/GaAs/Ge stack [1]. Another option, presently pursued for single junction cells, is modification of the spectrum by means of (spectral) down and/or up conversion or shifting. In case of downconversion an incident high-energy photon is converted into two or more lower energy photons; for upconversion two or more low energy photons (sub band gap) are converted into one high-energy photon. Downshifting is similar to downconversion where an important difference is that the quantum efficiency of the conversion process is unity, while that of shifting is lower than unity [2], although close to unity is preferred to minimize losses. Recent modelling studies on incorporation of conversion layers on top (downconverter or downshifter) or at the bottom (upconverter) of single junction solar cells have shown that the conversion efficiency may increase by about 10% [3–8]. Experimental work has shown a 6−% relative increase in conversion efficiency for coating a multi-crystalline silicon solar cell with a downshifting layer [9]. Coating of a CdS/CdTe solar cell with a layer that contained a fluorescent colouring agent was reported to lead to an increase of the spectral response in the blue, while a maximum increase in efficiency was calculated to be 30–40% [10].

Previously, we have modelled performance enhancement of solar cells resulting from inclusion of semiconductor nanocrystals or quantum dots (QDs) in a plastic layer on top of solar cells. Such layers may be denoted as downshifters (DSs). Modelling results showed a 10% increase in short circuit current under AM1.5 [7]. These results were based on existing designs of multicrystalline silicon solar cells, and the spectral downshifter properties (QD concentration and size) were optimized. Past, present and future cell designs have been compared [11], and it was shown that the improved cell designs were modelled to have a lower efficiency benefit from DS application than the older cell design: for the AM1.5G spectrum the current increase was 10, 8.5, and 7.5%, for the past, present, future cell design, respectively.

The efficiency of solar cells depends mainly on two irradiance properties, i.e., the irradiation intensity [12] and the spectral composition of incident light [13]. Both intensity and spectral composition vary depending on time (seasonal and daily variation), geographical location, presence of clouds, and air pollution. Simulating an annual performance of solar cells thus requires actual or typical irradiation distributions as input, e.g., for a particular location [14]. The short circuit current increase for DSs on top of solar cells for non-AM1.5 clear sky

E-mail address: w.g.j.h.m.vansark@chem.uu.nl.

0040-6090/$ - see front matter © 2007 Elsevier B.V. All rights reserved.
doi:10.1016/j.tsf.2007.12.080

spectra has been modelled to be larger (up to 30%) than for AM1.5 conditions [8]. It therefore is expected that annual performance increase of such devices is between 10 and 30%.

The present paper is a first attempt to estimate the performance of solar cells with DSs under realistic irradiation conditions, i.e., for varying spectral distributions as they may be found outdoors. The spectral distributions that we used for this evaluation were generated on a minutely basis by means of the spectrum simulation model SEDES2 [15]. Inputs for the model were minutely data for global, direct, and diffuse irradiation as well as other measured weather data from a meteorological measuring station in the Netherlands. The minutely spectra generated by the SEDES2 model were subsequently aggregated to yield hourly spectra, which are then used in modelling the output of the solar cell with and without DS. In this paper we will demonstrate the performance enhancement due to DSs for a number of typical days: a clear summer day, a cloudy summer day, a clear winter day, and a cloudy winter day.

2. Modelling approach

Two independent models were employed in this study. First, the SEDES2 spectral model was utilized to generate minutely spectral data. These spectra were aggregated to hourly data, and four typical days were selected. These spectra were applied in the calculation of solar cell performance using PC1D [16]. Results are compared for solar cells with and without spectral downshifter.

2.1. Spectral data simulation

Measured solar spectral data are not available in most countries, as also is the case for the Netherlands, due to the lack of spectral measurement stations. Therefore we modelled the spectra by employing the SEDES2 spectral model [15]. SEDES2 is an extension of SPCTRAL2 [17] that is able to model clear-sky spectra. SEDES2 includes modelling of spectra for cloudy skies, and was updated recently [18]. Required model inputs are total, diffuse and direct irradiance, ambient temperature, site's pressure, and relative humidity, on any time base. The spectra are calculated in the wavelength range of 300–1400 nm.

Since March 2005, the Royal Netherlands Meteorological Institute (KNMI) has established its own irradiance measurement station, which continuously records the total, diffuse, and direct irradiance every minute at geographical location of 51.971° N, 4.927° E in Cabauw, a location close to the city of Utrecht. These data are used in order to derive minutely simulated solar spectrum for a one year period from March 1st 2005 to February 28th 2006. Ambient temperature, relative humidity, and pressure were measured on site near (<100 m) to the irradiance measurement set-up. Spectra are calculated by SEDES2 for a 37° tilted surface directed towards the south. We thus can compare the spectra with the ASTM AM1.5G standard [19].

2.2. Solar cell configuration and simulation

The configuration studied is a highly transparent layer containing QDs on top of a solar cell (Fig. 1) [7]. Generally, the size of the QDs is taken such that both blue and green light is absorbed and emitted in the red, which corresponds to an optimum spectral response of the solar cell. Depending on the QD concentration also unabsorbed blue and green light enters the solar cell.

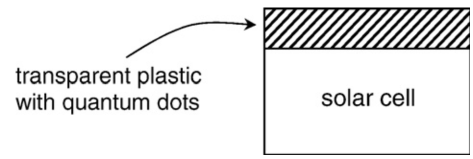

Fig. 1. Schematic drawing of the studied configuration. A plastic layer containing QDs is applied on top of a solar cell. Absorption of incident light and emission lead to a modified spectrum incident on the solar cell.

For solar cell simulation we use material and device parameters (status 2005 [20]) for the standard 12.5×12.5 cm^2 baseline n–p–p^+ mc-Si cell developed at the Energy research Centre of the Netherlands (ECN), which has parameters that are typical of low-cost commercial cells, including series resistance, shunt conductance and a second diode. The cell thickness is 300 µm, the cell has a shallow diffused emitter, and the 9 µm thick back-surface-field (BSF) has a p^+ surface doping level of 4×10^{18} cm^{-3}. The front surface anti-reflection coating consists of 71-nm thick silicon nitride with a refractive index $n=2.1$ deposited by means of an in-line Microwave Remote Plasma CVD process [21]. The performance of the solar cell is simulated with the simulation programme PC1D (version 5.8) [16], using incident spectra that are modified by the downshifting layer. The cell parameters without downshifter are: open circuit voltage 0.624 V, short circuit current 35.4 mA/cm^2, fill factor 0.773, efficiency 17.1%. The external collection efficiency of this solar cell is 0.62 at 400 nm, and 0.89 at 600 nm [11], the latter wavelength being the emission wavelength of the used quantum dots.

2.3. Spectrum modification

The incident spectrum, converted to amount of photons per wavelength $\Phi_s(\lambda)$, is modified by absorption of photons in the downshifting layer. The amount of absorbed photons in this layer $\Phi_a(\lambda)$ is determined from the QD absorption spectrum, which depends on the QD size, their concentration in the downshifting layer, and the thickness of this layer. This absorbed amount is subtracted from the incident spectrum: $\Phi_{sa}(\lambda)=\Phi_s(\lambda)-\Phi_a(\lambda)$. As the QDs re-emit light at a red-shifted wavelength, the amount of emitted photons $\Phi_e(\lambda)$ is calculated from the QD emission spectrum. To this end, a quantum efficiency (QE) of 0.8 [22] is assumed, as well as the assumption that 3/4 of the emitted photons is directed towards the underlying solar cell, due to internal reflection in the converter layer [23]. The amount of emitted photons is then added to the already modified spectrum: $\Phi_{sae}(\lambda)=\Phi_s(\lambda)-\Phi_a(\lambda)+\Phi_e(\lambda)$, and the resulting spectrum serves as input for the solar cell simulation models.

Absorption of photons is calculated by using the Lambert–Beer equation: the photon flux density $\Phi(x,\lambda)$ after passing a distance x in a film with absorption coefficient $\alpha(\lambda)$ is written as $\Phi(x,\lambda)=\Phi^0(\lambda)\exp[-\alpha(\lambda)x]$, with $\Phi^0(\lambda)$ the incident photon flux density. The exponential term $\alpha(\lambda)x$ equals $\varepsilon_\lambda CD$, with ε_λ the

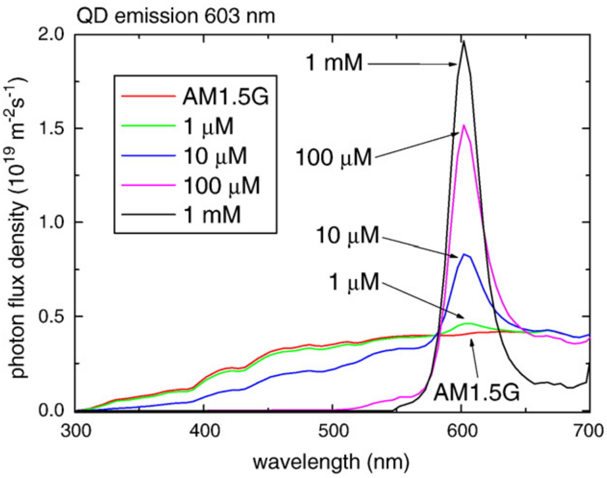

Fig. 2. Calculated modified AM1.5 global spectra for QD concentrations from 1 μM to 1 mM.

molar extinction coefficient (M^{-1} cm^{-1}), C the chromophore concentration (M), and D the thickness of the film (cm). The molar extinction coefficient is determined by scaling the normalized absorption spectrum such that the molar extinction coefficient ε_λ at 350 nm equals $\varepsilon_\lambda = 1.438 \times 10^{26}\ a^3$ [24]. The QD radius a is determined from the absorption maximum and the known relation with particle diameter [25]. The QD concentration varies from the nM to the mM range. The result of the procedure above for a QD emitting at 603 nm and an AM1.5 global incident spectrum is shown in Fig. 2. QD concentrations were varied from 1 nM to 10 mM at a downshifter D of 0.1 cm. Starting at a concentration of 1 μM an appreciable amount of photons is absorbed in the blue part of the spectrum, while the modified spectrum is increased at the QD emission wavelength. For concentrations >1 μM this effect clearly is much stronger. The effect of QD inclusion on all spectra is similar to the one shown in Fig. 2.

3. Results and discussion

3.1. Spectral data simulation

From over 200,000 spectra that were modelled four typical days were selected, representing the occurring extremes of variation in spectral composition in irradiation conditions during one year in the Netherlands: a clear summer day (19 June), a cloudy summer day (2 June), a clear winter day (25 December), and a cloudy winter day (11 December). Figs. 3 and 4 respectively show the spectra for these four days and their irradiation intensity as a function of time. The hourly spectra are constructed from

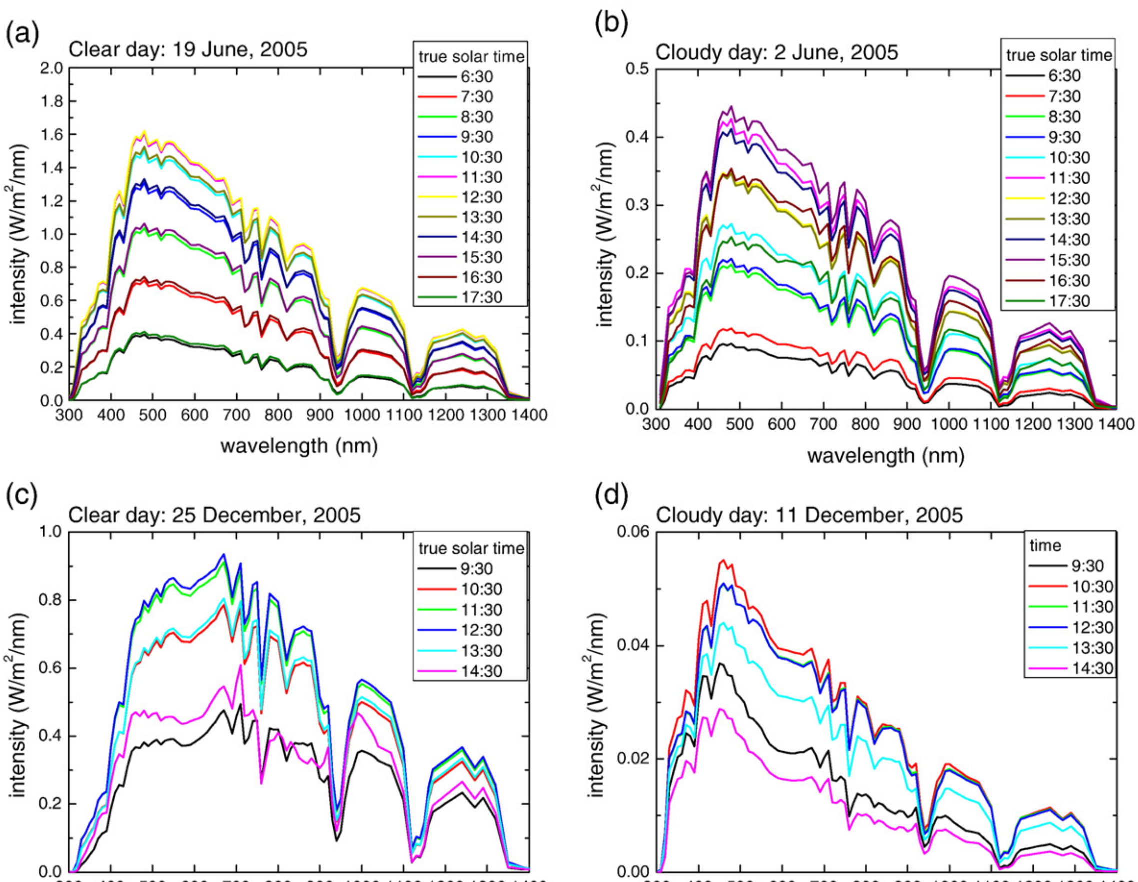

Fig. 3. Hourly spectra aggregated from calculated minutely spectra using SEDES2 and measured irradiation and meteorological data for four days. a) clear summer day (19 June); b) cloudy summer day (2 June); c) clear winter day (25 December); d) cloudy winter day (11 December). Hours are given in true solar time.

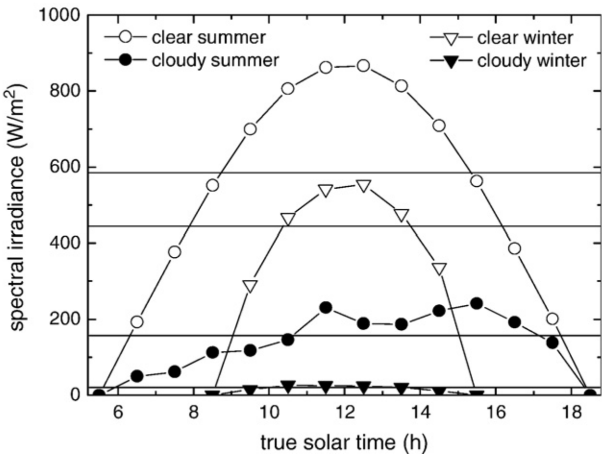

Fig. 4. Spectral irradiance variation as a function of true solar time for the four days as derived from Fig. 3. Average irradiances are indicated by the solid lines.

60 minutely spectra. The modelled spectra for the summer days were found to be similar to the ASTM AM1.5 standard. The weighted average photon energy (APE), calculated for the 300–1400 nm range, of the modelled clear and cloudy summer days varies between 1.71 and 1.77, which is only slightly higher than the 1.714 eV APE value that is found for the AM1.5 standard spectrum. Note that when using another spectral range, another APE is calculated: for example, Minemoto et al. used a range of 350–1050 nm and found a value of 1.878 eV as APE for the AM1.5 standard spectrum [26]. The APEs of the clear winter day are smaller than the AM1.5 value and vary between 1.55 and 1.61 eV, while the APEs of the cloudy winter day are larger and vary between 1.78 and 1.92 eV. The daily average spectral irradiances for the summer days are 585 W/m^2 (clear) and 157 W/m^2 (cloudy); for the winter days they are 444 W/m^2 (clear) and 20.4 W/m^2 (cloudy), as indicated in Fig. 4.

3.2. Solar cell simulation

Earlier work has revealed that the optimum QD concentration is 100 μM for a downshifter thickness of 1 mm and QDs emitting at 603 nm, for both AM1.5 and non-AM1.5 spectra [7,8], and also for different solar cell material quality [11]. We therefore used these data to calculate the cell's performance parameters.

Fig. 5 shows the simulated short circuit current as a function of true solar time for the four typical days comparing the downshifter without and with QDs. It is clear that the short circuit current is enhanced for all cases. The maximum current increase is 22.9% for the cloudy winter day at 14:30 h; the minimum current increase is 6.9% for the clear winter day at 8:30 h. Daily averages are shown in Table 1, and are compared with the APE. From the standard deviations in the mean for all but the cloudy winter day it is inferred that both APE and the short circuit current increase are not varying much over the course of the day. Also, the data in this table suggest a possible relation between average short circuit increase and APE; we therefore have plotted the relative short circuit current $J_{sc,rel}$ as a function of APE in Fig. 6. The data can well be fitted by means of the linear equation $J_{sc,rel}=a+b\times \text{APE}$, and we find $a=0.380\pm0.018$ and $b=0.436\pm0.011$. This apparent linear relationship may perhaps be used to calculate the short current increase using only the APE of all spectra throughout the year. However, we first will need to verify this relationship using spectra available for other days. This work is currently undertaken.

Note that the simulations do not take into account that the angle of incidence of irradiation varies over the course of the day; instead only normal incidence is studied. Non-normal incidence would increase absorption in the downshifter, leading to a somewhat larger emission at the emission wavelength, and

Table 1
Average photon energy (300–1400 nm) and short circuit current increase, with standard deviation of their means, for the four typical days indicated in Fig. 3

Day	Average photon energy (eV)	Average J_{sc} increase (%)
Clear summer	1.735±0.015	13.2±0.4
Cloudy summer	1.731±0.013	13.7±0.6
Clear winter	1.592±0.019	7.7±0.4
Cloudy winter	1.819±0.062	17.9±2.9

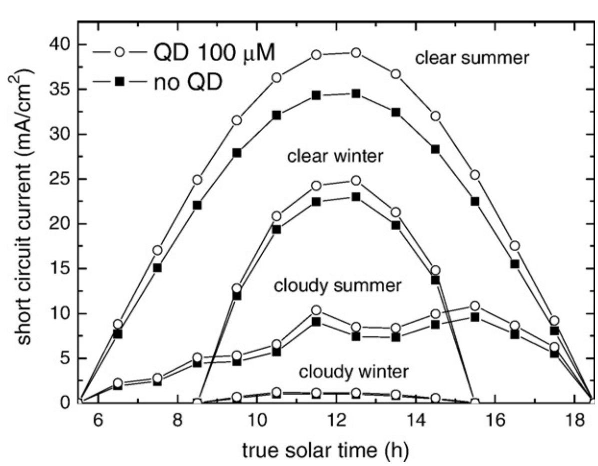

Fig. 5. Calculated short circuit current for the used solar cell with a downshifting layer with and without QDs. QD concentration is 100 μM, and emit at 603 nm. Downshifter thickness is 1 mm.

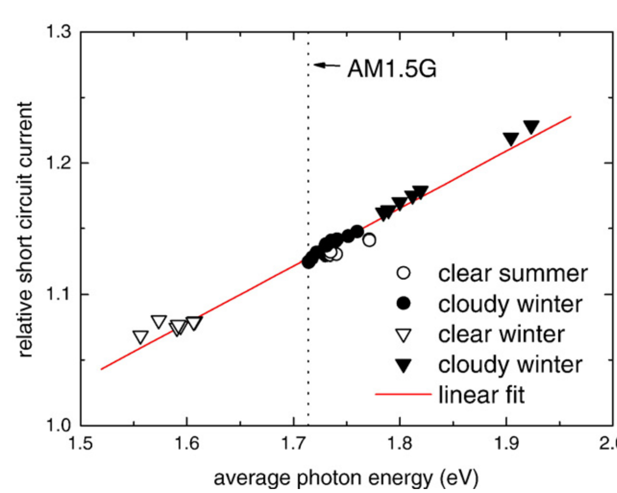

Fig. 6. Relative short circuit current increase as a function of average photon energy revealing a clear linear relationship.

consequently to a somewhat larger current increase. The simulations presented here thus reveal a conservative estimate of the current increase possibly to be attained including downshifters on top of solar cells.

4. Summary and conclusions

Performance enhancement in terms of short circuit increase of solar cells with a downshifter on their topside has been investigated using modelled spectra for four typical days throughout the year. These spectra can be characterized using the weighted average photon energy. A maximum short circuit increase of 22.9% is found for a cloudy winter day, corresponding to a high average photon energy value. A minimum short circuit increase of 6.9% is found for a clear winter day, corresponding to a low average photon energy value. Plotting the relative short current increase as a function of APE revealed a linear relationship. Current work is directed towards calculation of the annual performance of solar cells employing downshifting layers.

Acknowledgements

We gratefully acknowledge Bamshad Houshyani Hassanzadeh (UU) for extensive spectral modelling, Daryl Myers (National Renewable Energy Laboratory, NREL, USA) for enthusiastically updating SEDES2, Wouter Knap and Alexander Los (KNMI) for supplying Dutch irradiation data, Cees Tool and Arthur Weeber (Energy research Centre of the Netherlands (ECN)) for supplying cell design parameters, Nils Reich and Erik Alsema (UU) for critical reading of the manuscript, and the European Commission for financial support as part of the Framework 6 integrated project FULLSPECTRUM (contract SES6-CT-2003-502620).

References

[1] M.A. Green, K. Emery, D.L. King, Y. Hishikawa, W. Warta, Prog. Photovolt: Res. Appl. 15 (2007) 35.
[2] B.S. Richards, Sol. Energy Mater. Sol. Cells 90 (2006) 2329.
[3] B.S. Richards, Sol. Energy Mater. Sol. Cells 90 (2006) 1189.
[4] T. Trupke, A. Shalav, B.S. Richards, P. Wurfel, M.A. Green, Sol. Energy Mater. Sol. Cells 90 (2006) 3327.
[5] C. Strumpel, M. McCann, G. Beaucarne, V. Arkhipov, A. Slaoui, V. Svrcek, C. del Canizo, I. Tobias, Sol. Energy Mater. Sol. Cells 91 (2007) 238.
[6] G.C. Glaeser, U. Rau, Thin Solid Films 515 (2007) 5964.
[7] W.G.J.H.M. Van Sark, A. Meijerink, R.E.I. Schropp, J.A.M. Van Roosmalen, E.H. Lysen, Sol. Energy Mater. Sol. Cells 87 (2005) 395.
[8] W.G.J.H.M. Van Sark, Appl. Phys. Lett. 87 (2005) 151117.
[9] T. Maruyama, J. Bandai, J. Electrochem. Soc. 146 (1999) 4406.
[10] T. Maruyama, R. Kitamura, Sol. Energy Mater. Sol. Cells 69 (2001) 61.
[11] W.G.J.H.M. Van Sark, in: J. Poortmans, H. Ossenbrink, E. Dunlop, P. Helm (Eds.), Proceedings of the Twentyfirst European Photovoltaic Solar Energy Conference, Dresden, Germany, WIP, Munich, Germany, 2006, p. 155.
[12] N.H. Reich, W.G.J.H.M. Van Sark, E.A. Alsema, S.Y. Kan, S. Silvester, A.S.H. Van der Heide, R.W. Lof, R.E.I. Schropp, in: W. Hoffmann, J.-L. Bal, H. Ossenbrink, W. Palz, P. Helm (Eds.), Proceedings of the Twentieth European Photovoltaic Solar Energy Conference, Barcelona, Spain, WIP, Munich, Germany, 2005, p. 2120.
[13] S. Nann, K. Emery, Sol. Energy Mater. Sol. Cells 27 (1992) 189.
[14] W.G.J.H.M. Van Sark, Eur. J. Phys. 28 (2007) 415.
[15] S. Nann, C. Riordan, J. Appl. Meteorol. 30 (1991) 447.
[16] P.A. Basore, D.A. Clugston, in: D.J. Flood, J. Schmid, M. Yamaguchi (Eds.), Proceedings of the 25th IEEE Photovoltaic Specialists Conference, Washington, DC, USA, IEEE, 1996, p. 377.
[17] R.E. Bird, C. Riordan, J. Clim. Appl. Meteorol. 25 (1986) 87.
[18] D.R. Myers, private commun.
[19] ASTM, Standard Tables for Reference Solar Spectral Irradiances: Direct Normal and Hemispherical on 37° Tilted Surface, Standard G173-03e1, American Society for Testing and Materials, West Conshohocken, PA, USA, 2003.
[20] C.J.J. Tool, G. Coletti, F.J. Granek, J. Hoornstra, M. Koppes, E.J. Kossen, H.C. Rieffe, I.G. Romijn, A.W. Weeber, in: W. Hoffmann, J.-L. Bal, H. Ossenbrink, W. Palz, P. Helm (Eds.), Proceedings of the Twentieth European Photovoltaic Solar Energy Conference, Barcelona, Spain, WIP, Munich, Germany, 2005, p. 578.
[21] W. Soppe, H. Rieffe, A. Weeber, Prog. Photovolt: Res. Appl. 13 (2005) 551.
[22] L. Qu, X. Peng, J. Am. Chem. Soc. 124 (2002) 2049.
[23] A.J. Chatten, K.W.J. Barnham, B.F. Buxton, N.J. Ekins-Daukes, M.A. Malik, in: K. Kurokawa, L. Kazmerski, B. McNelis, M. Yamaguchi, C. Wronski, W.C. Sinke (Eds.), Proceedings of the Third World Congress on Photovoltaic Energy Conversion (WPEC-3), Osaka, Japan, 2003, p. 2657.
[24] C.A. Leatherdale, W.-K. Woo, F.V. Mikulec, M.G. Bawendi, J. Phys. Chem., B 106 (2002) 7619.
[25] B.O. Dabbousi, J. Rodriguez-Viejo, F.V. Mikulec, J.R. Heine, H. Mattoussi, R. Ober, K.F. Jensen, M.G. Bawendi, J. Phys. Chem., B 101 (1997) 9463.
[26] T. Minemoto, M. Toda, S. Nagae, M. Gotoh, A. Nakajima, K. Yamamoto, H. Takakura, Y. Hamakawa, Sol. Energy Mater. Sol. Cells 91 (2007) 120.